Scintillator performance was tested in different ways: Compatibility tests were performed at room temperature by placing SS304 metal strips in glass beakers filled with the scintillator samples and observing the color of the liquid, over a period of months. In order to obtain an overall picture of the scintillator performance, cylindrical cells of dimensions 1.5" by 5" diameter ("small cell") or 6.5" by 6" diameter ("large cell"), coupled to photomultipliers, were filled with the samples, and the light output response to γ-rays from a radio-active ^{22}Na source was measured. Fig. V.1 shows such ^{22}Na spectra for *BC-521* and two different batches of the *ND-309* scintillator, as measured with the large cell. For all three samples, one clearly observes the 0.34 and the 1.06 MeV Compton edges around channel numbers of 20 and 150, respectively.

Following these tests, scintillator emission spectra were measured, employing a *Perkin-Elmer* fluorescence spectro-photometer with a Xe lamp and monochromator providing light in a narrow band of wavelengths around 270 nm, the wavelength corresponding to the maximum absorbance of the scintillator. In addition, the absorption spectrum of each scintillator batch was measured with a *Perkin Elmer Lambda Six* absorption spectro-photometer, where a beam of polychromatic Xe light was passed through each sample and compared to the unattenuated direct light. Calibrations of the two spectrophotometers were checked, using a 10-3M antracene sample, dissolved in cyclohexane, or a holonium glass sample, respectively. The final acceptance test was performed with the NMM, filled with 360 gal of the scintillator to be tested.

The first batch ("Batch 1") of *ND-309* scintillator obtained from the company had a maximum in the emission spectrum which was red-shifted by 12 nm relative to *BC-521* and, therefore, not well matched to the photomultipliers. In addition, the light output was 30% lower than that of *BC-521*. More importantly, this scintillator turned out to be quite reactive even with SS304, leading to a significant discoloration of the liquid within only a few hours. The following Batch 2 and Batch 3 were custom made, with the particular application with the large *SuperBall* detector in mind. Their emission spectra are compared in Fig. V.2 with that of *BC-521* scintillator. As can be seen from this figure,

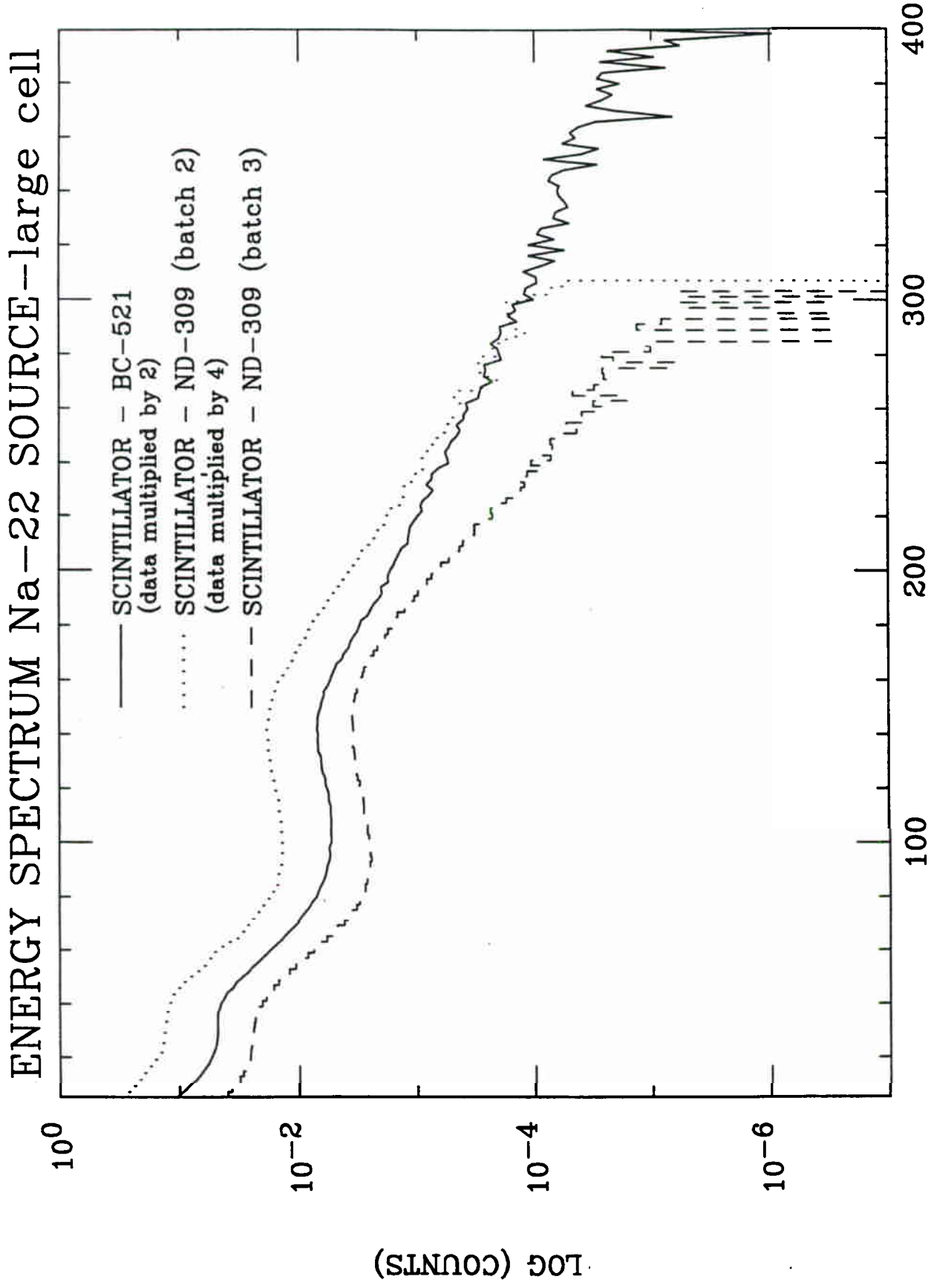

Fig. V.1: Energy spectra of a ^{22}Na γ-ray source obtained with a 6.5" x 6" diameter test cell containing BC-521 and two batches of ND-309 scintillator.

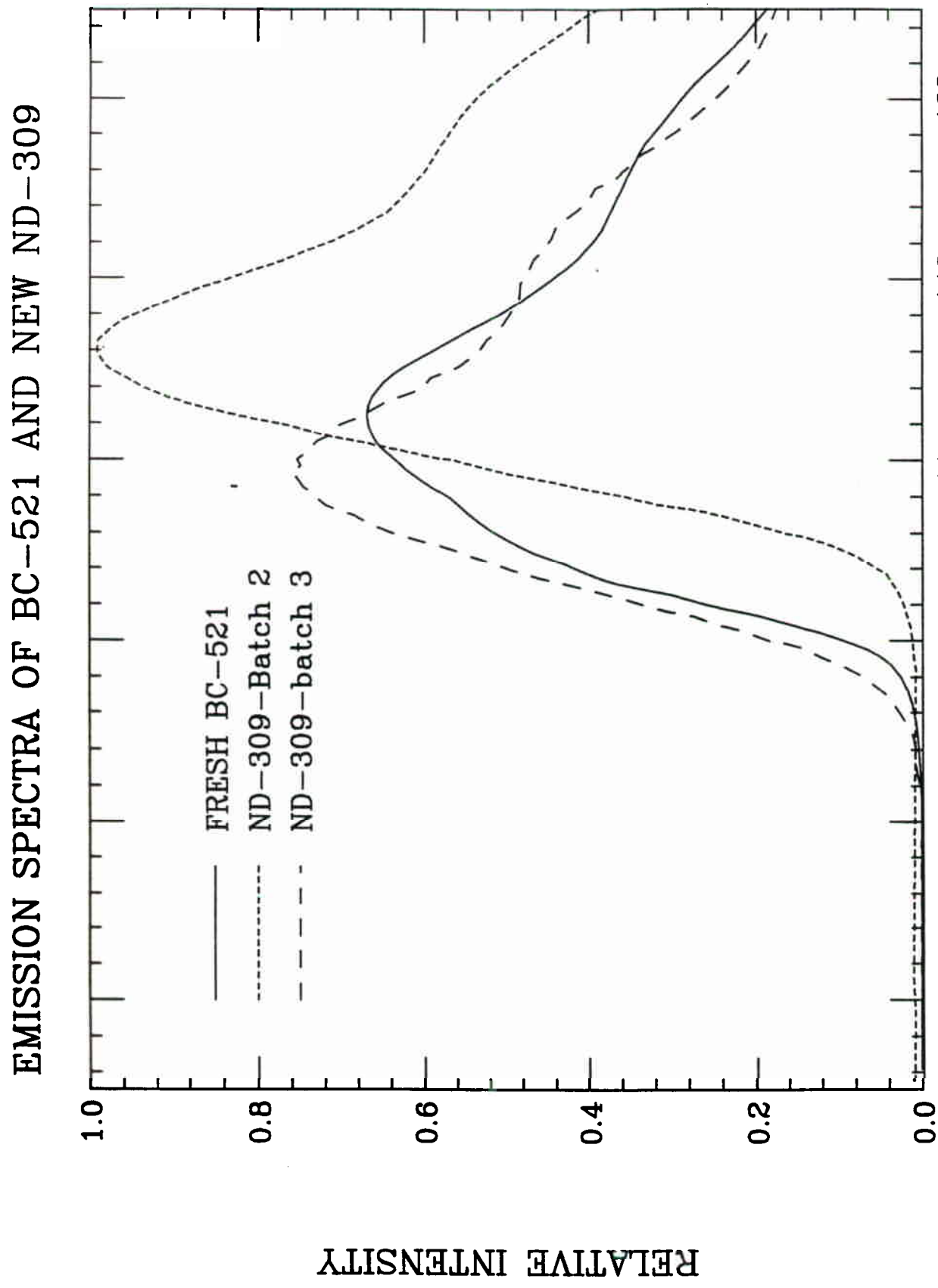

Fig. V.2: Emission spectra of BC-521 and two batches of ND-309 scintillator.

ND-309 Batch 2 had a 25% higher light output than *BC-521* but also an emission peak at too long a wave length (432 nm). The third (and final) Batch 3 of *ND-309*, which used the same formula but with the addition of wavelength shifters, shows an emission spectrum that, peaking at 418 nm, is better matched to the photomultiplier spectral sensitivity and has still a high light output.

In Fig. V.3, absorption spectra of two batches of *ND-309* are compared to those of a fresh sample of *BC-521* and one that had been used in the Rochester NMM, for a period of ten years. The purpose of measuring the absorption spectra is to determine the attenuation lengths of the different scintillators. If emission and absorption spectra of a scintillator overlap significantly, light emitted from the scintillator will be effectively reabsorbed by it, leading to a reduced useful light output. As seen from Fig. V.3, the absorption spectra of all samples are fairly similar, except for *ND-309* Batch 2, which, however, also has a red-shifted emission maximum. For the other samples, emission and absorption spectra overlap only in the tails of the distributions, as they should.

Since light is emitted almost isotropically from the luminiscence centers of the scintillator, only a fraction is seen directly by the photomultipliers. Most of the photons are emitted toward the tank walls, where they are either reflected or absorbed. Some initial tests with the large scintillator test cell confirmed that the coating of the wall surface is very important for an efficient light collection. Without any lining of the walls of this cell, both Compton edges seen in Fig. V.1 disappear in a broad and featureless light output spectrum. Therefore, measurements of the reflectance of several materials deemed suitable for a coating of the inner tank surfaces of the *SuperBall* were undertaken. Teflon and alumina sprays, aluminum coating and Teflon sheet lining were considered as alternatives, spanning a wide range in cost effectiveness.

Measurements of the diffuse reflectance of several materials were performed by *Hitachi Instruments Inc.*, using a spectro-reflectometer. This instrument is similar to a spectro-photometer but has a sphere integrating the (monochromatic) light reflected from

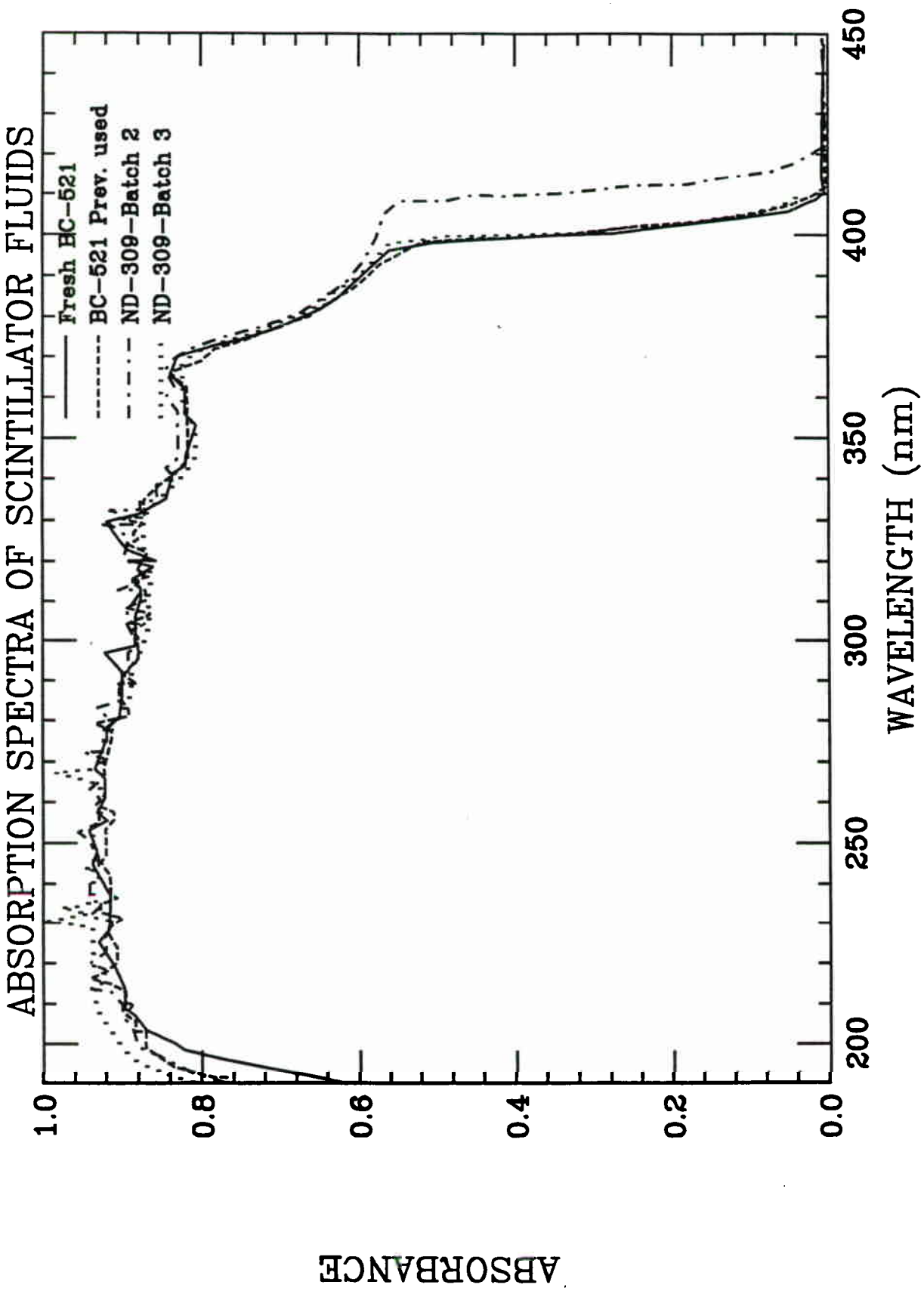

Fig. V.3: Absorption spectra of several batches of BC-521 and ND-309 scintillator.

the surface of a sample. Results are compared in Fig. V.4 to the reflectance achieved with an uncoated sheet of SS304. Here, a relative reflectance is plotted *vs* the wavelength of the light. From these results, one concludes that aluminum coating does not improve the reflectivity significantly, while both alumina and Teflon coating have large reflectances compared to bare steel. Clearly, Teflon coating or lining are the best, for the wavelength about the emission maximum of the scintillator. Since coating of the *SuperBall* inner tank surfaces with a spray-and-bake method was estimated as being time-consuming and expensive, a method of lining the tank walls with sheet Teflon tiles was adopted.

VI. Electronics

As discussed in the preceding sections, the operation of a neutron calorimeter based on the principles of fast neutron moderation, followed by neutron capture in Gd, requires the detection of a prompt response signal containing information on the total kinetic energy of a multiple-neutron event and many individual neutron capture signals, statistically dispersed over a time period of many μs. The prompt signal, hence, contains analog information requiring digitizing, while, in the simplest application, it is necessary to only count the number of capture signals, yielding the neutron multiplicity. However, it has been found useful, in previous applications of this method, to measure the time of detection of each capture event, relative to a time-zero defined by certain trigger detector, or relative to the neutron calorimeter's own prompt-response signal. For example, recording of such neutron capture times allows one to monitor multiple triggering or "cross-talk" between different *SuperBall* segments, where more than one segment detect a given capture event. It permits also, in the off-line data analysis, to optimize the length of the neutron counting interval with respect to the signal-to-background ratio. A special Five-Channel Multistop/Event Handler electronic module has been developed for this purpose.

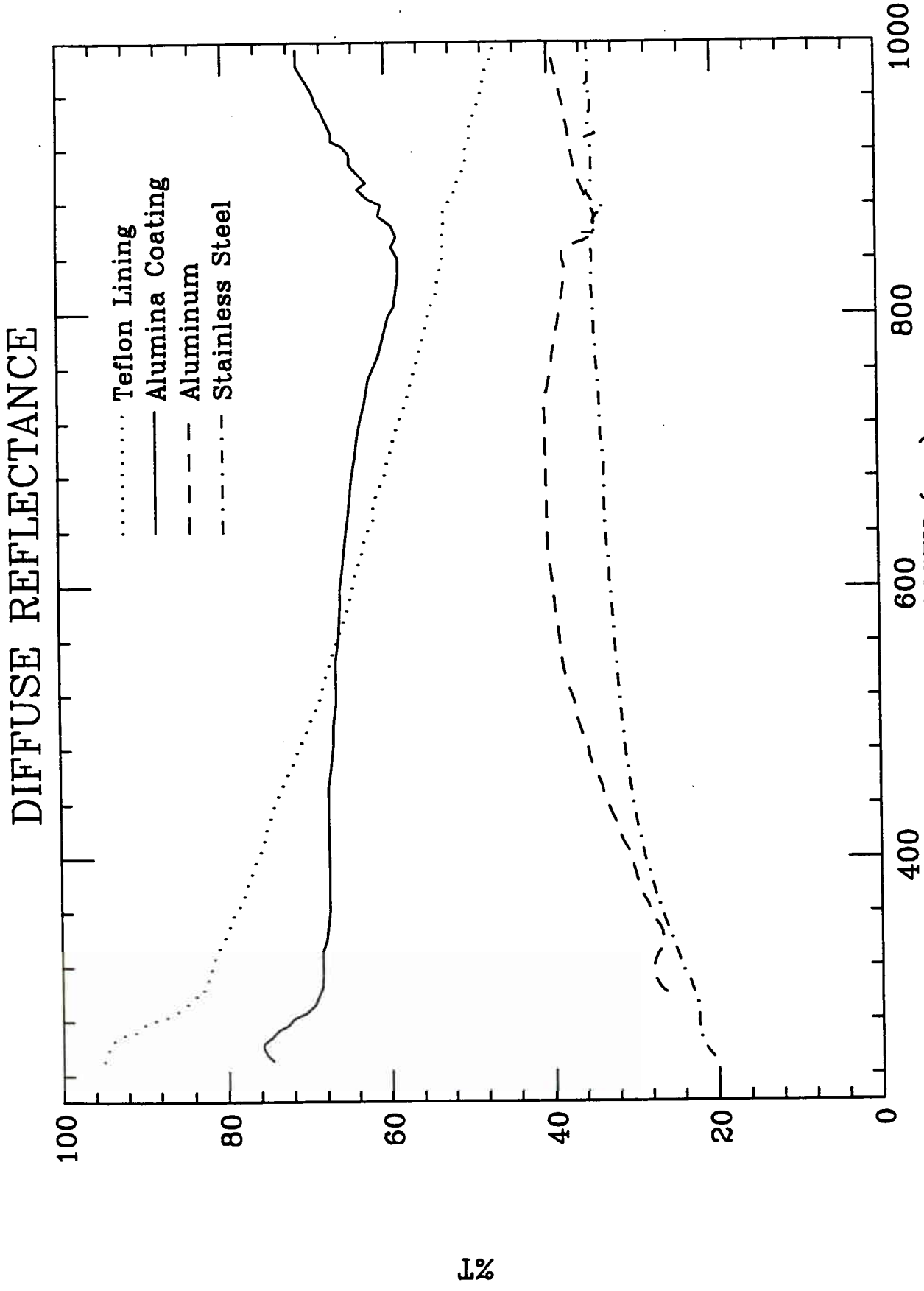

Fig. V.4: Diffuse reflectance measured with various linings of the test cell, plotted as a function of the wave length of the incident light.

To illustrate the task of the *SuperBall* counting electronics, the time sequence of events detected with the *SuperBall* is illustrated in Fig. VI.1. Here, t = 0 is the time of a reaction event produced in the target (Trace A in Fig. VI.1), as signaled by some kind of trigger detector, typically a Si detector telescope. The *SuperBall* tanks show a prompt response, the first pulse on Trace B, due to reaction γ-rays and fast neutron scattering in the scintillator, followed by a number of delayed pulses due to neutron capture or background events. The first pulse is selected by a coincidence with a valid signal from the trigger detector. Delayed by approximately 200 ns, it acts as a "start" signal (Trace C) for the neutron event handling and counting process. It triggers a 128- μs long counting gate pulse (Trace D) for counting the neutron multiplicity, a 300- μs long veto or busy signal (Trace E), used for blocking the electronics against multiple triggers, and a prompt gate pulse (Trace F), used to enable a charge (or amplitude)-to-digital converter Q(A)DC measuring the prompt-response analog signal. Delayed pulses are accepted, as long as they fall into the period of gate pulse D, as valid neutron (or background) events (Trace G). These pulses provide successive stop signals for the Multistop-TDC/Event Handler. Each delayed neutron capture also generates a "neutron" pulse (Trace H) for gating a QDC measuring the delayed light output associated with a neutron capture, i.e., the capture- γ-ray spectrum. The background is measured in a similar fashion as the delayed neutrons, but this measurement is triggered randomly, if not coinciding with the measurement of a reaction event in progress.

The *SuperBall* electronic apparatus processes signals from the 52 *Thorn-EMI* 9390KB07 photomultipliers of the detector. This photomultiplier type has been designed for high-resolution applications; it is medium-fast, with a pulse rise time of ~ 10 ns. It has a bialkali cathode and 10 dynodes. Positive high voltage is provided to the TB1108 bases by a dedicated *LeCroy* System 1440 multi-channel HV supply. The commercial TB1108 bases have been modified to include a single-transistor preamplifier stage for the photomultiplier anode signals, to be operated in series with the voltage divider chain. The circuit boosts anode signals such that they can be used directly, and without further amplification, for the generation of logical signals. These anode signals can be used, for ex-

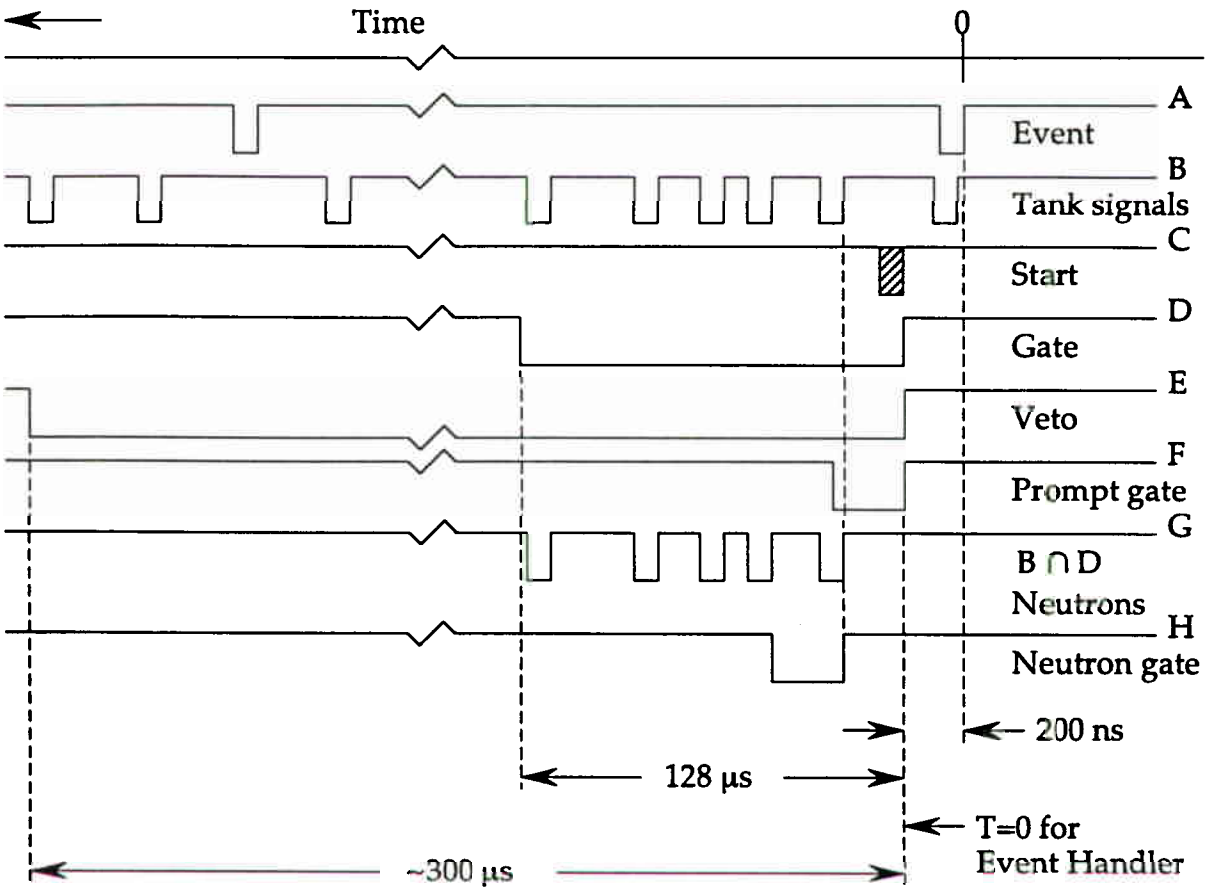

Fig. VI.1: The time sequence of events detected with the *SuperBall.*

ample, as inputs to the 16-channel constant-fraction timing discriminators MSU-1806, developed by *LeCroy* for the APEX experiment and acquired also for the *SuperBall*.

A simplified block diagram of the schematics of the specialized *SuperBall* electronics is given in Fig. VI.2. Here, the boosted Anode signals feed directly into 16-channel Constant Fraction Discriminators, whose output signals can be used for triggering a "hit pattern" unit identifying the photomultipliers that have fired in an event. This information is useful for determining the azimuthal angular distribution of the incident neutrons and for an on-line monitoring of the photomultiplier performance. In the somewhat simplified electronics scheme used in the first *SuperBall* test and production experiments, only analog and timing information derived from the fast signals from the 10th dynode have been utilized. A specialized module has been built for each *SuperBall* tank, representing the contents of the box in Fig. VI.2, except for the CFD's. In this electronics scheme, the dynode signals of all (8 or 12) photomultipliers of a given *SuperBall* tank are first summed in a fast analog Sum/Invert unit. This summed signal provides the prompt and delayed light output information of that tank, the prompt part of which is digitized by a gated Analog-to-Digital Converter. This summed signal is also used to define the electronic threshold for the detection of the capture γ-rays, which determines the neutron detection efficiency. It is amplified (Fast Amp.) and triggers a leading-edge discriminator (Disc.). The delayed logical output signals from this discriminator provide the stop signals for the Multi-Stop Time-to-Digital Converter measuring the capture times of all neutrons in a tank. The converter is started by a signal generated from the coincidence (Logic) between any of the five tank timing signals and a signal from a trigger detector. This latter signal also indicates a valid reaction event in the *SuperBall* calorimeter.

In order to process the signal streams from the *SuperBall* in an effective and economic fashion, a dedicated CAMAC module, the Five-Channel Multistop TDC/Event Handler, has been designed and built, which replaces a whole array of expensive commercial electronics modules. The module implements to a large extent programmable array logic technology and is capable of recording, event by event with 250-ns precision and 25-ns

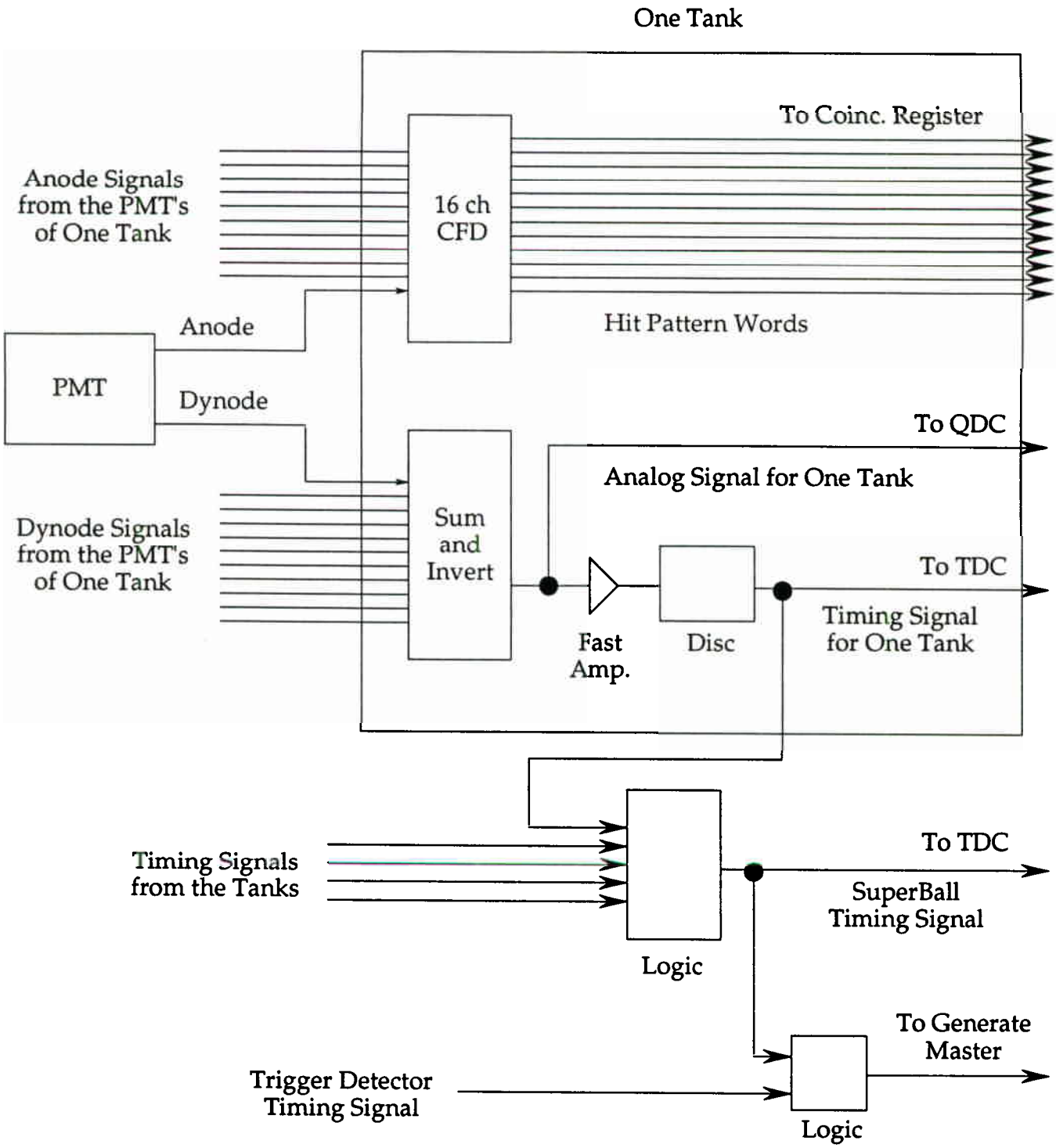

Fig. VI.2: Block diagram of SuperBall electronics.

dead time, the arrival times of up to 512 signals, separately for each of the five segments of the *SuperBall* and for the detector as a whole. Independently, the module counts the multiplicities of signals arriving at each of the five inputs, as well as the multiplicities of logical OR signals for five selected combinations of inputs.

The principle of operation is illustrated by the block diagram shown in Fig. VI.3. Each acquisition cycle of the module is started by a signal (START) arriving at the LOGICS MASTER controller. This signal is represents the time of a reaction event. The MASTER starts a tunable clock and enables arrays of ten multiplicity COUNTERs and six FIFO memories. It also disables its START input, to prevent multiple triggering and sends busy signals to front-panel dead time output (DT) and LED indicator (B). The clock signal is applied to the inputs of the programmable binary TIMER COUNTER and the GREY CODER. The GREY CODER output is sent onto the CLOCK-WRITE bus of the FIFO's, for storage in the respective FIFO upon arrival of the shift-in (SI) signals. The latter signals are produced by individual multiplicity COUNTERs in response to each valid STOP input signals, for each of the five *SuperBall* tanks, and for combinations of them. The acquisition cycle continues until the binary TIMER COUNTER reaches its limit determined by TIMER PRESET switches. Then, and end-of-acquisition signal is sent to the LOGIC MASTER, who disables COUNTERs and FIFOs, generates a LAM signal for the CAMAC bus, and sends a ready signal to a front panel output (INT OUT). The module then stores in its five FIFOs the Grey-coded binary representations of the times of arrival of STOP signals and stores its ten COUNTERs the multiplicity counts for the various individual signals and signal combinations. Subsequent readout of COUNTERs and FIFOs is achieved through execution of corresponding CAMAC function commands. Upon completion of readout, the module can be cleared either by an external fast CLEAR or a CAMAC clear command.

The above development of specialized electronic modules, replacing numerous commercial devices and accessories, has allowed to simplify the dedicated *SuperBall* electronics setup considerably, in comparison to the original concept. The remainder of the elec-

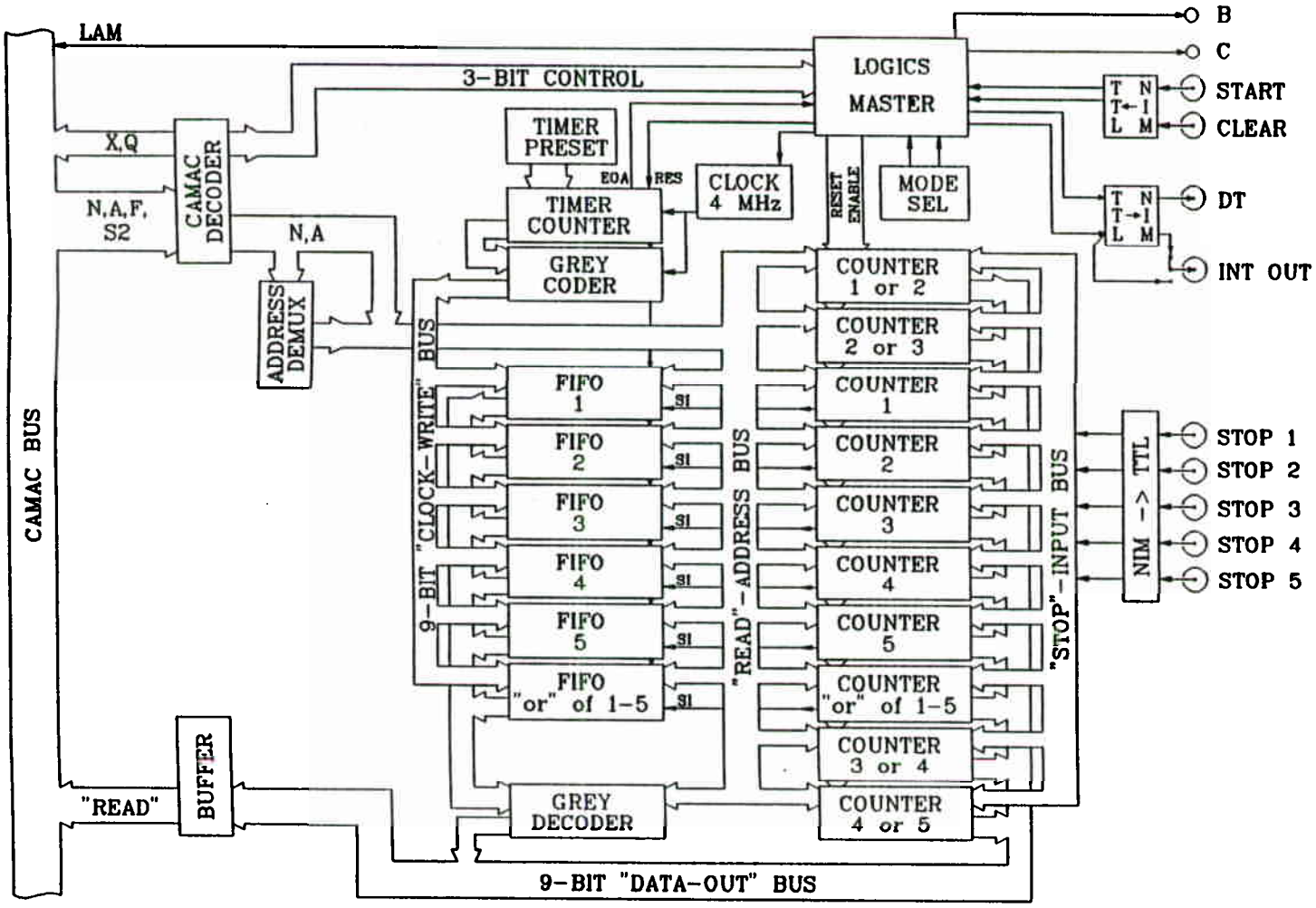

Fig. VI.3: Block diagram of the Multistop-TDC/Event Handler.

tronic setup is assembled from conventional NIM and CAMAC modules available in the general electronics pools of typical accelerator facilities.

VII. *SuperBall* Construction and Installation

The tank segments, undercarriages, rails, and the auxiliary maintenance tank were manufactured by *Fab-Alloy Inc.* in Jackson, Michigan, with Ms. K.M. Levy as supervising engineer of the construction project. Parts of the scattering chamber, the flanges of the photomultiplier windows, the photomultiplier housings, the rails, and many other miscellaneous parts for the *SuperBall* were made or modified by Mr. D. Quinn and Mr. C.L. Carr in the University of Rochester Department of Chemistry mechanical workshops. The order (RC-147819-F) for the *SuperBall* tanks with undercarriages was placed with *Fab-Alloy Inc.* on February 2, 1993, and the detector was delivered at the National Superconducting Cyclotron Laboratory on September 15, 1993.

The individual tanks are manufactured by *Fab-Alloy Inc.* from sections of 1/4" stainless-steel SS304 pipes and sheets, formed to cylindrical, conical, or spherical shapes. The end pieces of each tank were constructed from dished heads of standard sizes available to *Fab-Alloy* from other vendors. This construction principle is illustrated in Fig. VII.1 showing two views of one of the conical end tank segments (1 and 5). The outer shell of either of these two tanks carries 8 photomultiplier ports. Some of the stainless-steel flanges of the tank are visible in the upper portion of Fig. VII.1. These flanges are attached to the shells of the tanks with full-penetration welds. In the view of the segment displayed in the lower part of the figure, the three sections of which the cone is fabricated are clearly defined by the connecting welds. Tank segment 3 is shown in Fig. VII.2, with its "negative" cone seen at the top left of the figure. In the assembled and docked configuration, this cone will accept the "positive" counterpart of segment 4 (cf. Fig. IV.5).

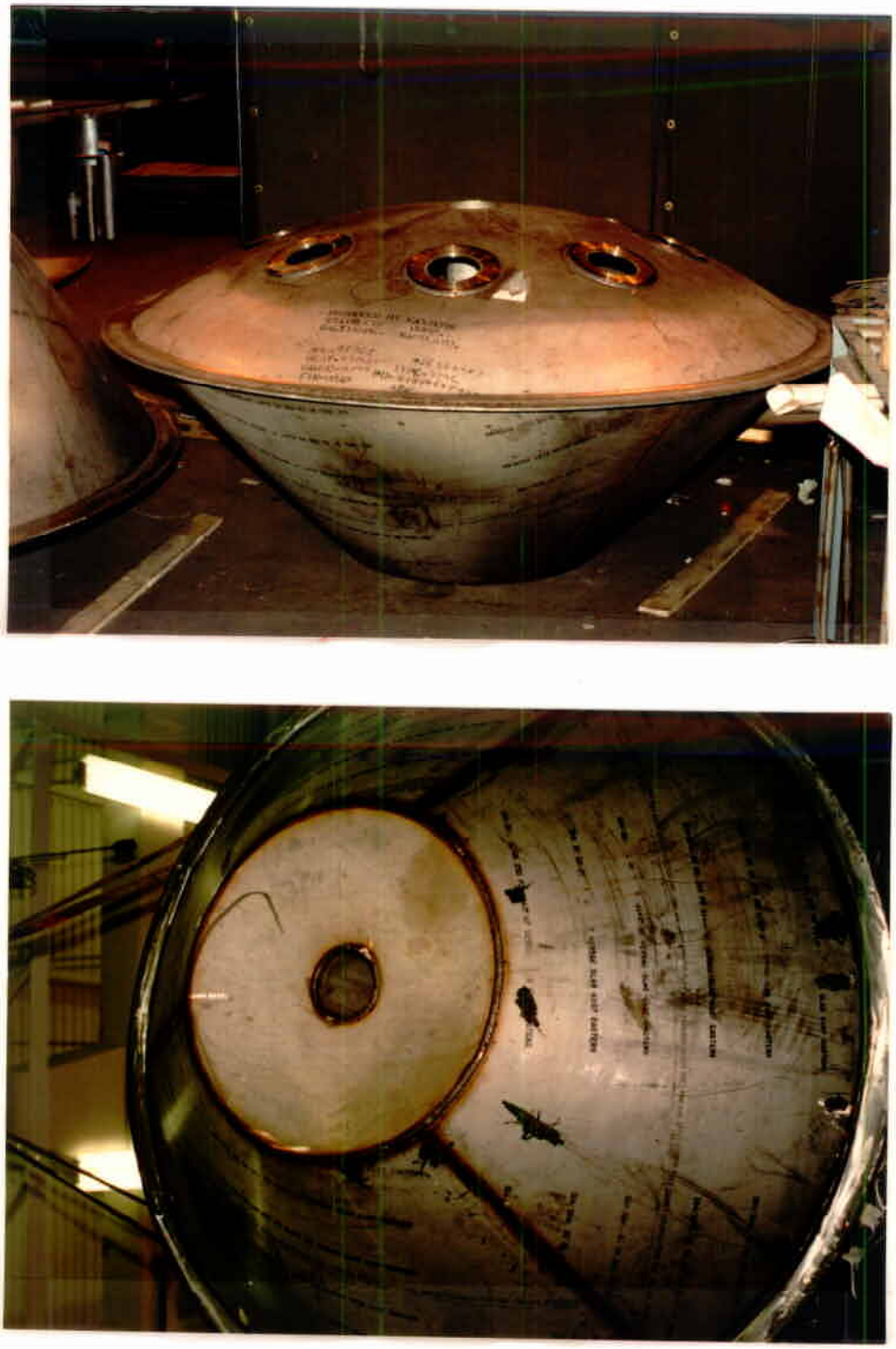

Fig. VII.1: Two views of one of the conical end tank segments (1 and 5). The outer shell of either of these two tanks carries 8 photomultiplier ports. Some of the stainless-steel flanges of the tank are visible in the upper portion of the figure.

Fig. VII.2: Tank segment 3 with its "negative" cone is seen at the top. The photomultiplier ports are blanked off for transport and testing.